

## Microscopic Based Density Matrix Treatments of Electron-Transfer Reactions in Condensed Phases

Chienyu F. Jen and Arieh Warshel\*

Department of Chemistry, University of Southern California, Los Angeles, California 90089

Received: April 21, 1999; In Final Form: September 15, 1999

Several non-phenomenological density matrix treatments of electron-transfer (ET) reactions in condensed phases are developed and examined. The methods consider the donor and acceptor system (the solute) under the influence of the surrounding fluctuating solvent. The main emphasis is placed on semiclassical methods, where the starting point is the Hamiltonian of the quantum mechanical electronic states of the solute. The diagonal elements of the Hamiltonian include the fluctuations of the solute electronic energies as a result of the interaction between the solute and the field from the classically moving solvent molecules. The fluctuating Hamiltonian is used to construct a Liouville equation, which is treated by three approaches. The first method is based on a direct numerical integration of the relevant Liouville equation. The second involves the use of a second-order Liouville equation, and the third involves the use of a Redfield type equation. The methods are examined by simulating electron transfer between two sodium-like atoms that are held at a 4 Å separation in water. The simulations generate the fluctuations of the electronic energies of the states that are involved in the electron-transfer process. The fluctuating energies are then used in evaluating the rate constant of the reaction as a function of its assumed free energies. The results of the three approaches are similar to the corresponding results obtained from the Marcus equation. However, the Redfield equation converges much more quickly than the direct Liouville equation and its second-order version. The problems associated with the semiclassical treatments are briefly considered, emphasizing the approximation involved in treating the solvent motion classically. Some of these problems can be overcome by a previously developed density matrix approach<sup>1</sup> that uses classical simulations to evaluate the Franck–Condon factors of the solvent vibronic states. This vibronic density matrix treatment is briefly described and used in simulating an electron-transfer reaction in the reaction center from *Rps. viridis*.

### I. Introduction

Many fundamental processes in chemistry and biology involve charge-transfer reactions in condensed phases.<sup>2</sup> Understanding such processes on a detailed microscopic level is of great current interest,<sup>2–5</sup> and significant progress has already been made by computer simulation approaches.<sup>1,2,6–12</sup> This includes the simulations of electron transfer (ET) in the diabatic and adiabatic limits<sup>2,10–12</sup> and simulations of proton transfer (PT) and other processes in the adiabatic limit.<sup>2,13–16</sup> Yet simulations that describe consistently the time evolution of more than two electronic states in solutions in the diabatic, adiabatic, and the intermediate limits have not been fully developed and examined. Such approaches are clearly needed for systems with intermediate coupling, and a good example is the case of the primary charge separation in bacterial reaction centers. This case involves three electronic states with coupling whose exact magnitude is unknown, but its estimates are in the upper end of the diabatic limit.

In the search for an effective approach for simulating multi-level crossing processes in dissipative systems, it is tempting to explore the density matrix approach. This approach has been developed to what is perhaps the most powerful tool for studying relaxation processes on a phenomenological level.<sup>17–19,23–28</sup> It is not obvious, however, how to incorporate microscopic simulations of charge-transfer processes in density matrix treatments. For example, semiclassical models that treat the electronic states

quantum mechanically and the solvent motion classically can result in density matrix treatments that violate the rule of microscopic reversibility. Another problem may be associated with the description of the solute–solvent coupling.<sup>7</sup> Some density matrix treatments may not reproduce correctly the effect of the change of the solute dipole moment on the solvent “reaction field”. Furthermore, semiclassical density matrix approaches cannot provide exact quantum mechanical results for transitions between electronic states due to the classical description of the solvent modes. Trying to treat the solvent modes quantum mechanically leads to major problems with regards to the evaluation of the relevant relaxation time  $T_1$  that describes the vibrational relaxation within each electronic state. That is, in simpler problems, such as vibrational relaxation of diatomic molecules in solution, it is quite easy to obtain the  $T_1$  for transitions between the solute vibrational levels from MD simulations by considering the perturbation of the solute vibrational level by the solvent fluctuations. However, it is not clear how to do so in simulations of charge-transfer processes when  $T_1$  describes transitions between the solvent vibrational levels to themselves. In such cases, the solvent is both the relaxing system and the system that causes the relaxation.

The present work develops, examines, and compares different ways of combining MD simulations with density matrix treatments. The focus of this work is on semiclassical treatments where the electronic states are described quantum mechanically and the solvent nuclear motions (vibrational states) are treated

classically. Nevertheless, a quantum mechanical treatment of the solvent vibrational modes is also considered.

## II. Semiclassical Theoretical Treatments

This section develops and examines alternative density matrix models for simulations of surface crossing processes in condensed phases. The models considered include a direct Liouville treatment, a second-order Liouville treatment, and a Redfield type formalism. The performance of the different models in studies of charge-transfer processes in polar solvents is used as a validity check.

We will confine a significant part of our derivation to a simple model of only two electronic states, considering an electron transfer from a donor D to an acceptor A in a polar solvent. However, the formulation used can be easily extended to cases with many electronic states. The time-independent wave function of a two-state system can be approximated by a combination of the diabatic wave functions

$$\begin{aligned}\phi_a^i &= \varphi(\text{D}) \varphi(\text{A}^+) \psi_{\text{solvent}}^{i,a} = \varphi_a \psi_{\text{solvent}}^{i,a} \\ \phi_b^j &= \varphi(\text{D}^+) \varphi(\text{A}) \psi_{\text{solvent}}^{j,b} = \varphi_b \psi_{\text{solvent}}^{j,b}\end{aligned}\quad (1)$$

where  $\psi$  is the combined wave function of the solvent molecules with  $i$  and  $j$  designating different electronic states of these wave functions. Neglecting charge transfer from the solute to the solvent, we can treat the effect of solvent excitations by assigning classical induced dipoles to its molecules while omitting the  $i$  and  $j$  indexes (e.g., see the appendix of ref 33). Thus, the time-dependent wave function of the system can be approximated by

$$\Psi(\mathbf{x}, \mathbf{Q}, \mathbf{R}, t) = C_a(t) \varphi_a(\mathbf{x}) + C_b(t) \varphi_b(\mathbf{x}) \quad (2)$$

where  $\mathbf{x}$ ,  $\mathbf{Q}$ , and  $\mathbf{R}$  are the coordinate vectors of the solute electrons, the solvent nuclei, and the solute nuclei, respectively. Here, we consider a case where both the distance between A and B and the solute coordinates are fixed (if needed, we can treat the vibrations of the solute quantum mechanically). In this case the time-dependent wave function can be written as

$$\Psi(\mathbf{x}, t) = C_a(\mathbf{Q}(t)) \varphi_a(\mathbf{x}) + C_b(\mathbf{Q}(t)) \varphi_b(\mathbf{x}) \quad (3)$$

The time evolution of the system can be determined by solving the time-dependent Schrödinger equation while integrating over the electronic wave function. This gives

$$\dot{C} = \frac{i}{\hbar} H C \quad (4)$$

where the vector  $\mathbf{C}$  is given by  $(C_a(t), C_b(t))$  and the effective two-state Hamiltonian is given by

$$\mathbf{H}(\mathbf{Q}) = \begin{bmatrix} H_{aa}(\mathbf{Q}) & \sigma(\mathbf{Q}) \\ \sigma(\mathbf{Q}) & H_{bb}(\mathbf{Q}) \end{bmatrix} \quad (5)$$

where  $H_{\alpha\beta} = \langle \varphi_\alpha | H | \varphi_\beta \rangle$ ,  $\epsilon_\alpha^0 = H_{\alpha\alpha}$ , and  $\sigma = H_{ab}$ . In our specific case we can write

$$\mathbf{H}(t) = \begin{bmatrix} \epsilon_a^0 + U_a(Q(t)) & \sigma \\ \sigma & \epsilon_b^0 + U_b(Q(t)) \end{bmatrix} \quad (6)$$

where  $U_i$  represents the time-dependent interaction between the

solute and the fluctuating solvent molecules. In cases where  $\sigma$  is large it might be required to move to the adiabatic representation in order to get stable time-dependent integration. This requires diagonalization of the Hamiltonian in every time step and consideration of the solvent-induced fluctuations of the adiabatic energies (for a related treatment in surface hopping studies see ref 8). However, the points examined in the present paper are more conveniently discussed in the diabatic representation. Issues that are related to the transfer from the diabatic to the adiabatic limits are left to subsequent studies (see also discussion in section III). At any rate, within the diabatic representation of eq 6 we can write the Hamiltonian as

$$\begin{aligned}\mathbf{H}(t) &= \begin{bmatrix} \epsilon_a^0 & 0 \\ 0 & \epsilon_b^0 \end{bmatrix} + \begin{bmatrix} U_a(t) & 0 \\ 0 & U_b(t) \end{bmatrix} + \begin{bmatrix} 0 & \sigma \\ \sigma & 0 \end{bmatrix} \\ &= H^0 + H^+(t) \\ &= H^0 + H^U(t) + H(\sigma)\end{aligned}\quad (7)$$

In this work we chose to use a density matrix approach rather than to solve eq 4. Thus, we consider the Liouville equation

$$\dot{\rho} = \frac{i}{\hbar} \{ \rho \mathbf{H}(t) - \mathbf{H}(t) \rho \} = \frac{i}{\hbar} [ \rho, \mathbf{H} ] \quad (8)$$

where  $\rho_{\alpha\beta} = C_\alpha C_\beta^*$

Many times it is convenient to use the interaction representation where  $\rho$  and  $\mathbf{H}$  are transformed into the following matrices.

$$\rho^*(t) = \exp\{ (i/\hbar) \mathbf{H}^0 t \} \rho(t) \exp\{ -(i/\hbar) \mathbf{H}^0 t \} \quad (9)$$

$$\mathbf{H}^{+*}(t) = \exp\{ (i/\hbar) \mathbf{H}^0 t \} \mathbf{H}^+(t) \exp\{ -(i/\hbar) \mathbf{H}^0 t \}$$

The time dependence of  $\rho^*$  is obtained by solving

$$\dot{\rho}^* = \frac{i}{\hbar} [ \rho^*, \mathbf{H}^{+*}(t) ] \quad (10)$$

The calculation of the actual population of the system requires the evaluation of the ensemble average of  $\rho$ , using

$$\langle \rho^*(\tau) \rangle_0 = \langle \int_0^\tau \dot{\rho}^*(t) dt \rangle_0 \quad (11)$$

where  $\langle \rangle_0$  designates an average over the initial conditions of the system. Here, we will try first to examine a second-order approach that follows the approximations made in deriving the Redfield equation. In this strategy one avoids the direct numerical averaging of the Liouville equation by performing short time averages on the second-order density matrix. That is, for a finite but short time interval we can write<sup>17</sup>

$$\begin{aligned}\langle \rho^*(\tau) \rangle_0^{(2)} &= \left\langle \frac{i}{\hbar} [ \rho^*(t_0), \mathbf{H}^{+*}(t) ] + \right. \\ &\quad \left. \left( \frac{i}{\hbar} \right)^2 \int_{t_0}^\tau [ [ \rho^*(t_0), \mathbf{H}^{+*}(t') ], \mathbf{H}^{+*}(t) ] dt' \right\rangle_0\end{aligned}\quad (12)$$

In an explicit numerical integration we update the second-order equation every time step, using

$$\begin{aligned}\langle \rho^*(t_n) \rangle_0^{(2)} &= \left\langle \frac{i}{\hbar} [ \rho^*(t_{n-1}), \mathbf{H}^{+*}(t) ] + \right. \\ &\quad \left. \left( \frac{i}{\hbar} \right)^2 \cdot \int_{t_{n-1}}^{t_{n-1} + \Delta t} [ [ \rho^*(t_{n-1}), \mathbf{H}^{+*}(t') ], \mathbf{H}^{+*}(t) ] dt' \right\rangle_0\end{aligned}\quad (13)$$

Here, the formal expression of eq 12, which corresponds to a single time step, is replaced by the corresponding prescription

in an iterative numerical integration. This means that  $t$  is replaced by  $t_n$  and  $\rho^*(t_0)$  is replaced by  $\rho^*(t_{n-1})$ . Of course, this expression is used only in numerical integration and not in formal one step derivations (where eq 12 is being used).

Next we expand eq 12 and obtain

$$\begin{aligned} \langle \hat{\rho}_{\alpha\alpha}^*(t) \rangle_0^{(2)} &= \left\langle \frac{i}{\hbar} [\rho^*(t_0), \mathbf{H}^{+*}(t)] \right\rangle_0 + \\ &\frac{1}{\hbar^2} \sum_{\beta\beta'} \int_{t_0}^t \{ \langle H_{\alpha\beta}^+(t') H_{\beta'\alpha}^+(t) \rho_{\beta\beta'}^*(t_0) \rangle_0 e^{i(\alpha-\beta)t'} e^{i(\beta'-\alpha)t} + \\ &\langle H_{\alpha\beta}^+(t) H_{\beta'\alpha}^+(t') \rho_{\beta\beta'}^*(t_0) \rangle_0 e^{i(\beta'-\alpha)t'} e^{i(\alpha-\beta)t} - \\ &\langle \rho_{\alpha\beta}^*(t_0) H_{\beta\beta'}^+(t') H_{\beta'\alpha}^+(t) \rangle_0 e^{i(\beta-\beta')t'} e^{i(\beta'-\alpha)t} - \\ &\langle \rho_{\beta'\alpha}^*(t_0) H_{\alpha\beta}^+(t) H_{\beta\beta'}^+(t') \rangle_0 e^{i(\beta-\beta')t'} e^{i(\alpha-\beta)t} \} dt' \quad (14) \end{aligned}$$

Here, we denoted in the exponents  $\epsilon_\alpha$  by  $\alpha$  and  $\epsilon_\beta$  by  $\beta$ . This simplified notation is also used elsewhere.<sup>17</sup> We also use the relationship<sup>17</sup>

$$H_{\alpha\beta}^*(t) = e^{i(\alpha-\beta)t} H_{\alpha\beta}(t) \quad (15)$$

$$\rho_{\alpha\beta}^*(t) = e^{i(\alpha-\beta)t} \rho_{\alpha\beta}(t)$$

In the explicit expansion of eq 14 we will use the relationship

$$\langle \alpha | H^U | \beta \rangle = H_{\alpha\beta}^U = \delta_{\alpha\beta} U_\alpha \quad (16)$$

$$\langle \alpha | H^\sigma | \beta \rangle = H_{\alpha\beta}^\sigma = (1 - \delta_{\alpha\beta}) \sigma_{\alpha\beta}$$

$$\langle H_{\alpha\beta}^U(t) H_{\gamma\delta}^U(t') \rangle_0 = \delta_{\alpha\beta} \delta_{\gamma\delta} \langle U_\alpha(t) U_\gamma(t') \rangle_0$$

Rather than continuing with this general equation, we focus here on the simplest case of the two-state system where we can write

$$\begin{aligned} \langle \hat{\rho}_{aa}^*(t) \rangle_0^{(2)} &= \frac{i}{\hbar} \langle (\rho_{ab}^*(t_0) \sigma_{ba}^* - \sigma_{ab}^* \rho_{ba}^*(t_0)) \rangle_0 - \\ &\frac{1}{\hbar^2} \sum_{\beta\beta'} \int_{t_0}^t \{ \langle \rho^*(t_0) \mathbf{H}^{+*} \tilde{\mathbf{H}}^{+*} - \tilde{\mathbf{H}}^{+*} \rho^*(t_0) \mathbf{H}^{+*} - \\ &\mathbf{H}^{+*} \rho^*(t_0) \tilde{\mathbf{H}}^{+*} + \tilde{\mathbf{H}}^{+*} \mathbf{H}^{+*} \rho^*(t_0) \rangle_0 dt' \quad (17) \end{aligned}$$

$$\begin{aligned} \langle \hat{\rho}_{ab}^*(t) \rangle_0^{(2)} &= \frac{i}{\hbar} \langle [\rho_{ab}^*(t_0) \Delta U_{ba}(t) + \sigma_{ab}^* (\rho_{aa}^*(t_0) - \rho_{bb}^*(t_0))] \rangle_0 - \\ &\frac{1}{\hbar^2} \int_{t_0}^t \{ \langle \rho^*(t_0) \mathbf{H}^{+*} \tilde{\mathbf{H}}^{+*} - \tilde{\mathbf{H}}^{+*} \rho^*(t_0) \mathbf{H}^{+*} - \\ &\mathbf{H}^{+*} \rho^*(t_0) \tilde{\mathbf{H}}^{+*} + \tilde{\mathbf{H}}^{+*} \mathbf{H}^{+*} \rho^*(t_0) \rangle_0 dt' \end{aligned}$$

where  $\mathbf{H}$  and  $\tilde{\mathbf{H}}$  designate the Hamiltonian at time  $t$  and  $t'$ , respectively.

After some manipulations we obtain

$$\begin{aligned} \langle \hat{\rho}_{aa}^*(t) \rangle_0^{(2)} &= \frac{i}{\hbar} \langle (\rho_{ab}^*(t_0) \sigma_{ba} e^{i(b-a)t} - \rho_{ba}^*(t_0) \sigma_{ab} e^{i(a-b)t}) \rangle_0 - \\ &\frac{1}{\hbar^2} \int_{t_0}^t dt' \{ [\sigma^2 [e^{i(a-b)(t-t')} + e^{i(b-a)(t-t')}] \langle \rho_{aa}^*(t_0) - \rho_{bb}^*(t_0) \rangle_0 + \\ &[\langle \Delta U_{ba}(t') (\rho_{ab}^*(t_0) \sigma_{ba} e^{i(b-a)t} + \rho_{ba}^*(t_0) \sigma_{ab} e^{i(a-b)t}) \rangle_0] \} \quad (18) \end{aligned}$$

$$\begin{aligned} \langle \hat{\rho}_{ab}^*(t) \rangle_0^{(2)} &= \frac{i}{\hbar} \langle [\rho_{ab}^*(t_0) \Delta U_{ba}(t) + \sigma_{ab} e^{i(a-b)t} \times \\ &(\rho_{aa}^*(t_0) - \rho_{bb}^*(t_0)) \rangle_0 + \frac{1}{\hbar^2} \int_{t_0}^t dt' \{ [2\sigma_{ab}^2 e^{2i(a-b)t} \rho_{ba}^*(t_0) - \\ &2\sigma_{ab} \sigma_{ba} \rho_{ab}^*(t_0)] \rangle_0 - \langle \Delta U_{ba}(t) \sigma_{ab} e^{i(a-b)(t-t')} \times \\ &[\rho_{aa}^*(t_0) - \rho_{bb}^*(t_0)] \rangle_0 - [\langle \rho_{ab}^*(t_0) \Delta U_{ba}(t) \Delta U_{ba}(t') \rangle_0] \} \end{aligned}$$

where  $(a-b)$  is a shorthand notation for  $(\epsilon_a^0 - \epsilon_b^0)$ ,  $\Delta U_{ba}(t) = U_b(t) - U_a(t)$  and where we introduce the constraint  $\langle \Delta U_{ba}(t) \rangle_0 = 0$  by choosing the proper  $\epsilon_a^0$  and  $\epsilon_b^0$ . Equation 18 will be considered in a direct evaluation of the second-order Liouville equation.

Next we try to obtain a simpler expression for eq 18. We do so by manipulating the second-order Liouville equation in the way used in deriving the Redfield equation. Our task is to express eq 14 in an autocorrelation formalism. In this derivation we followed ref 17 and use for convenience the expression

$$J_{\alpha\alpha\beta\beta'}(\omega) = \int_{-\infty}^{\infty} \langle H_{\alpha\alpha}^+(t') H_{\beta\beta'}^+(t) \rangle_0 e^{-i\omega(t-t')} dt' \quad (19)$$

We start by noting that eq 14 has terms of the form

$$\begin{aligned} &\sum_{\beta\beta'} \int_0^{t-t'} dt' \langle H_{\alpha\beta}^+(t') H_{\beta'\alpha}^+(t) \rangle_0 e^{-i(\alpha-\beta)(t-t')} e^{i(\alpha-\beta+\beta'-\alpha)t} \\ &= \sum_{\beta\beta'} \langle \int_0^\infty H_{\alpha\beta}^+(t') H_{\beta'\alpha}^+(t) e^{-i(\alpha-\beta)(t-t')} dt' \rangle_0 e^{i(\alpha-\beta+\beta'-\alpha)t} \quad (20) \end{aligned}$$

$$\cong \frac{1}{2} \sum_{\beta\beta'} \int_{-\infty}^\infty dt' \langle H_{\alpha\beta}^+(t') H_{\beta'\alpha}^+(t) \rangle_0 e^{-i(\alpha-\beta)(t-t')} e^{i(\alpha-\beta+\beta'-\alpha)t}$$

where we extend the integration limit to infinity, since the autocorrelation is assumed to decay in a relatively short time.

Following ref 17 we assume that the complex parts are negligible so that

$$\begin{aligned} &\frac{1}{2} \sum_{\beta\beta'} \int_{-\infty}^\infty dt' \langle H_{\alpha\beta}^+(t') H_{\beta'\alpha}^+(t) \rangle_0 e^{-i(\alpha-\beta)(t-t')} e^{i(\alpha-\beta+\beta'-\alpha)t} \\ &= \sum_{\beta\beta'} \left[ \frac{1}{2} \int_{-\infty}^\infty dt' \langle H_{\alpha\beta}^+(t) H_{\beta'\alpha}^+(t') \rangle_0 \left( \frac{1}{2} \{ e^{-i(\alpha-\beta)(t-t')} + \right. \right. \\ &\left. \left. e^{i(\alpha-\beta)(t-t')} \} \right) \right] e^{i(\alpha-\beta+\beta'-\alpha)t} \quad (21) \end{aligned}$$

$$= \frac{1}{4} \sum_{\beta\beta'} [J_{\alpha\alpha\beta'\beta}(\alpha - \beta) + J_{\alpha\alpha\beta\beta'}(\beta - \alpha)] e^{i(\alpha-\beta+\beta'-\alpha)t}$$

Thus, for example,

$$\begin{aligned} &\frac{1}{2} \int_{-\infty}^\infty dt' \langle H_{ab}^+(t') H_{bb}^+(t) \rangle_0 e^{-i(a-b)(t-t')} e^{i(a-b)t} = \\ &\frac{1}{2} \int_{-\infty}^\infty dt' \langle \sigma U_b(t) \rangle_0 e^{-i(a-b)(t-t')} e^{i(a-b)t} \quad (22) \end{aligned}$$

Here, we neglect the complex part of  $e^{-i(a-b)(t-t')}$ , which is equal to  $-i \sin[(\epsilon_a^0 - \epsilon_b^0)(t-t')]$  because the sine term approaches zero as  $t-t' \rightarrow 0$ . Thus, we have

$$\begin{aligned}
e^{-i(a-b)(t-t')} &\cong \cos[(a-b)(t-t')] & (23) \\
&= \frac{1}{2} \{ \cos[(a-b)(t-t')] + \cos[(b-a)(t-t')] \} \\
&= \frac{1}{2} [e^{i(a-b)(t-t')} + e^{-i(a-b)(t-t')}]
\end{aligned}$$

Now we can rewrite eq 22 as

$$\begin{aligned}
\frac{1}{2} \int_{-\infty}^{\infty} dt' \langle \sigma U_b(t) \rangle_0 & \left[ \frac{1}{2} \{ e^{i(a-b)(t-t')} + e^{-i(a-b)(t-t')} \} \right] e^{i(a-b)t} = \\
& \frac{1}{4} [J_{abbb}(a-b) + J_{abbb}(b-a)] e^{i(a-b)t} \quad (24)
\end{aligned}$$

With this and  $\langle \Delta U_{ba}(t) \rangle_0 = 0$ , we can write eq 18 as

$$\begin{aligned}
\langle \dot{\rho}_{aa}^*(t) \rangle_0^{(2)} &= \frac{i}{\hbar} \langle (\rho_{ab}^*(t_0) \sigma_{ba} e^{i(b-a)t} - \rho_{ba}^*(t_0) \sigma_{ab} e^{i(a-b)t}) \rangle_0 - \\
& \frac{1}{2\hbar^2} \sigma_{ab}^2 \langle \rho_{aa}^*(t_0) - \rho_{bb}^*(t_0) \rangle_0 \int_{-\infty}^{\infty} dt' [e^{i(a-b)(t-t')} + e^{i(b-a)(t-t')}] = \\
& \frac{i}{\hbar} \langle (\rho_{ab}^*(t_0) \sigma_{ba} e^{i(b-a)t} - \rho_{ba}^*(t_0) \sigma_{ab} e^{i(a-b)t}) \rangle_0 \quad (25)
\end{aligned}$$

$$\begin{aligned}
\langle \dot{\rho}_{ab}^*(t) \rangle_0^{(2)} &= \frac{i}{\hbar} \langle [\rho_{ab}^*(t_0) \Delta U_{ba}(t) + \sigma_{ab} e^{i(a-b)t} (\rho_{aa}^*(t_0) - \\
& \rho_{bb}^*(t_0))] \rangle_0 + \frac{1}{2\hbar^2} \int_{-\infty}^{\infty} dt' \{ \langle [2\sigma_{ab}^2 e^{2i(a-b)t} \rho_{ba}^*(t_0)] \rangle_0 - \\
& \langle \rho_{ab}^*(t_0) \rangle_0 \langle \Delta U_{ba}(t) \Delta U_{ba}(t') \rangle_0 \} = \frac{i}{\hbar} \sigma_{ab} e^{i(a-b)t} \langle [\rho_{aa}^*(t_0) - \\
& \rho_{bb}^*(t_0)] \rangle_0 - \frac{1}{2\hbar^2} \langle \rho_{ab}^*(t_0) \rangle_0 \int_{-\infty}^{\infty} dt' [\Delta U_{ba}(t) \Delta U_{ba}(t')] \rangle_0
\end{aligned}$$

where we used the fact that

$$\int_{-\infty}^{\infty} dt' e^{i(a-b)t'} = \int_{-\infty}^{\infty} dt' \cos[(\epsilon_a^0 - \epsilon_b^0)t'] = 0$$

Equation 25 is our final expression for the second-order Liouville equation.

The next approach considered in this work is a direct use of the Redfield formulation. In doing so we add to the standard relaxation term the  $\sigma$ 's terms that do not exist in Redfield's treatment. This leads to a modified Redfield expression

$$\begin{aligned}
\dot{\rho}_{\alpha\alpha'}^*(t) &= \sum_{\beta\beta'} R_{\alpha\alpha'\beta\beta'} e^{i(\bar{\alpha}-\bar{\alpha}'-\bar{\beta}+\bar{\beta}')t} \rho_{\beta\beta'}^*(t_0) + \frac{i}{\hbar} \sum_{\beta} [\rho_{\alpha\beta}^*(t_0) \\
& \sigma_{\beta\alpha'} e^{i(\bar{\beta}-\bar{\alpha}')t} (1 - \delta_{\beta\alpha'}) - \sigma_{\alpha\beta} \rho_{\beta\alpha'}^*(t_0) e^{i(\bar{\alpha}-\bar{\beta})t} (1 - \delta_{\alpha\beta})] \quad (26)
\end{aligned}$$

The elements of the  $\mathbf{R}$  matrix are given by

$$\begin{aligned}
R_{\alpha\alpha'\beta\beta'} &= \frac{1}{2\hbar^2} [J_{\alpha\beta\alpha'\beta'}(\bar{\alpha}' - \bar{\beta}') + J_{\alpha\beta\alpha'\beta'}(\bar{\alpha} - \bar{\beta}) - \\
& \delta_{\alpha\beta'} \sum_{\gamma} J_{\gamma\beta\gamma\alpha'}(\bar{\gamma} - \bar{\beta}) - \delta_{\alpha\beta} \sum_{\gamma} J_{\gamma\alpha'\gamma\beta'}(\bar{\gamma} - \bar{\beta}')] \quad (27)
\end{aligned}$$

In our  $2 \times 2$  test case we obtain

$$\begin{aligned}
R_{aaaa} &= \frac{1}{2\hbar^2} [2J_{aaaa}(0) - J_{aaaa}(0) - J_{baba}(b-a) - J_{aaaa}(0) - \\
& J_{baba}(b-a)] = 0 \quad (28)
\end{aligned}$$

since  $J_{baba}(b-a) = 0$ ,

$$R_{bbaa} = \frac{1}{2\hbar^2} [2J_{bbaa}(b-a) - \delta_{ba} - \delta_{ba}] = 0 \quad (28)$$

$$R_{aabb} = \frac{1}{2\hbar^2} [2J_{aabb}(a-b) - \delta_{ab} - \delta_{ab}] = 0$$

$$\begin{aligned}
R_{abab} &= \frac{1}{2\hbar^2} [2J_{aabb}(0) - J_{aaaa}(0) - J_{baba}(b-a) - \\
& J_{abab}(a-b) - J_{bbbb}(0)] \\
&= \frac{1}{2\hbar^2} [2J_{aabb}(0) - J_{aaaa}(0) - J_{bbbb}(0)] - \\
& \frac{1}{2\hbar^2} [J_{baba}(b-a) + J_{abab}(a-b)] \\
&= \frac{1}{2\hbar^2} \int_{-\infty}^{\infty} [2\langle U_a(0) U_b(t) \rangle_0 - \langle U_a(0) U_a(t) \rangle_0 - \\
& \langle U_b(0) U_b(t) \rangle_0] dt - \frac{1}{2\hbar^2} \int_{-\infty}^{\infty} 2\sigma^2 dt \\
&= -\frac{1}{2\hbar^2} \int_{-\infty}^{\infty} \langle \Delta U_{ba}(0) \Delta U_{ba}(t) \rangle_0 dt = -\frac{1}{T_2}
\end{aligned}$$

$$\begin{aligned}
R_{abaa} &= \frac{1}{2\hbar^2} [2J_{aaba} - J_{abaa} - J_{bbba}] \\
&= \frac{1}{2\hbar^2} \int_{-\infty}^{\infty} \langle 2U_a(t) \sigma - \sigma U_a(t) - U_b(t) \sigma \rangle_0 dt \\
&= -\frac{1}{2\hbar^2} \int_{-\infty}^{\infty} \{ \langle \Delta U_{ba}(t) \rangle_0 \sigma \} dt = 0
\end{aligned}$$

$$R_{abbb} = \frac{1}{2\hbar^2} \int_{-\infty}^{\infty} \{ \langle \Delta U_{ba}(t) \rangle_0 \sigma \} dt = 0$$

$$R_{abba} = \frac{1}{2\hbar^2} [J_{abba}(b-a) + J_{abba}(a-b)]$$

$$= \frac{1}{2\hbar^2} \int_{-\infty}^{\infty} 2\sigma^2 dt = 0$$

Now we can write

$$\begin{aligned}
\langle \dot{\rho}_{aa}^*(t) \rangle_0 &= R_{aaaa} \rho_{aa}^*(t_0) + R_{aaab} e^{i(b-a)t} \rho_{ab}^*(t_0) + \\
& R_{aaba} e^{i(a-b)t} \rho_{ba}^*(t_0) + R_{aabb} \rho_{bb}^*(t_0) + \\
& \frac{i}{\hbar} \langle [\rho_{ab}^*(t_0) \sigma_{ba} e^{i(b-a)t} - \sigma_{ab} e^{i(a-b)t} \rho_{ba}^*(t_0)] \rangle_0 \quad (29) \\
&= \frac{i}{\hbar} \langle [\rho_{ab}^*(t_0) \sigma_{ba} e^{i(b-a)t} - \rho_{ba}^*(t_0) \sigma_{ab} e^{i(a-b)t}] \rangle_0
\end{aligned}$$

$$\begin{aligned}
\langle \dot{\rho}_{ab}^*(t) \rangle_0 &= R_{abab} \langle \rho_{ab}^*(t_0) \rangle_0 + R_{abba} e^{2i(a-b)t} \langle \rho_{ba}^*(t_0) \rangle_0 + \\
& R_{abaa} e^{i(a-b)t} \langle \rho_{aa}^*(t_0) \rangle_0 + R_{abbb} e^{i(a-b)t} \langle \rho_{bb}^*(t_0) \rangle_0 + \\
& \frac{i}{\hbar} \langle [\rho_{aa}^*(t_0) \sigma_{ab} - \sigma_{ab} \rho_{bb}^*(t_0)] e^{i(a-b)t} \rangle_0
\end{aligned}$$

$$= +\frac{i}{\hbar} \sigma_{ab} e^{i(a-b)t} \langle [\rho_{aa}^*(t_0) - \rho_{bb}^*(t_0)] \rangle_0 - \frac{1}{T_2} \langle \rho_{ab}^*(t_0) \rangle_0$$

Comparing eq 29 and 25, we see that the only difference is the last term in eq 25. Equations 29 and 25 will become identical once we assume that

$$\begin{aligned} & \langle \rho_{ab}^*(t_0) \int_{-\infty}^{\infty} dt' [\Delta U_{ba}(t) \Delta U_{ba}(t')] \rangle_0 \\ & \cong \langle \rho_{ab}^*(t_0) \rangle_0 \int_{-\infty}^{\infty} dt' \langle \Delta U_{ba}(t) \Delta U_{ba}(t') \rangle_0 \\ & = \frac{\langle \rho_{ab}^*(t_0) \rangle_0}{T_2} \end{aligned}$$

This approximation is partially an ad hoc approximation, since it is essential for obtaining the simple  $T_2$  expression for Redfield's treatment. However, it is reasonable to assume that  $\rho_{ab}(t_0)$ , which depends on the way the system is prepared, is not correlated strongly with  $\Delta U_{ba}(t)$ . The approximation used here can be also used in the second-order Liouville equation. We left this equation, however, in the form of eq 25 in order to help clarify why the use of the Redfield equation is faster than the use of the first- and second-order Liouville equation. The reason is, of course, that in the Redfield treatment we evaluate  $T_2$  once while in the second-order Liouville treatment we keep evaluating the  $\Delta U \times \Delta U$  product at each time step in the integration of  $\rho^*(t)$ .

One may wonder at this point why our treatment does not have a formal  $T_1$  term for the relaxation between the solvent modes. The reason is that our semiclassical treatment treats classically the relaxation between the vibrational modes of the same electronic state. This relaxation is obtained automatically in the MD simulations. The validity of this treatment is established in the next section where we show that we reproduce the correct microscopic reversibility relationship.

### III. Comparing Different Treatments

Equation 29 is not identical to eq 25 because of the use of different approximations. Thus, it is not clear if they give physically correct results. In particular, it is not obvious that the resulting forward and backward rate constants satisfy the requirement of microscopic reversibility. An effective way to check the validity of the different expressions is to examine whether the results reproduce Marcus' relationship for well-defined test cases. Here, we considered as a test case an electron transfer between a sodium-like ion and a sodium-like atom ( $\text{Na}^+ + \text{Na} \rightarrow \text{Na} + \text{Na}^+$ ) in water. The simulations were done using the program ENZYMIK<sup>34</sup> and applying the surface constraint all-atom solvent (SCAAS) spherical model<sup>20,35</sup> with a sphere radius of 20 Å. The long-range forces were treated consistently by the local reaction field (LRF) approach.<sup>36</sup> The van der Waals parameters for the sodium–water interaction were taken from ref 20, and the donor–acceptor pair was held at 4.0 Å apart, assuming that the electronic coupling is  $1 \text{ cm}^{-1}$  (i.e.,  $\sigma = 1 \text{ cm}^{-1}$ ). The rate constant of electron transfer between these two ions was evaluated using our umbrella sampling/free energy perturbation approach.<sup>8,20</sup> The relevant data were generated by running trajectories over 11 mapping potentials that took the system gradually from the reactant to the product state (see ref 20 for more details about this procedure). The trajectories were propagated with 1 fs time steps at 300 K. Each of the 11 mapping steps involved 40 ps simulation time. The resulted time-dependent energy gap,  $\Delta U_{ba}(t)$ , and its autocorrelation are given in Figure 1. The rate constants generated by the simulated  $\Delta U(t)$  depend on the assumed  $\Delta G_0$  (or  $\epsilon_b^0 - \epsilon_a^0$ ). This  $\Delta G_0$  can be shifted in a parametric way from its zero value to any other value. Thus, our study is not confined to the  $\text{Na}^+ - \text{Na}$  system but to hypothetical sodium-like spherical atoms with the same solute–solvent interaction energies as the Na and  $\text{Na}^+$  but with different ionization energy and thus different  $\Delta G_0$ .

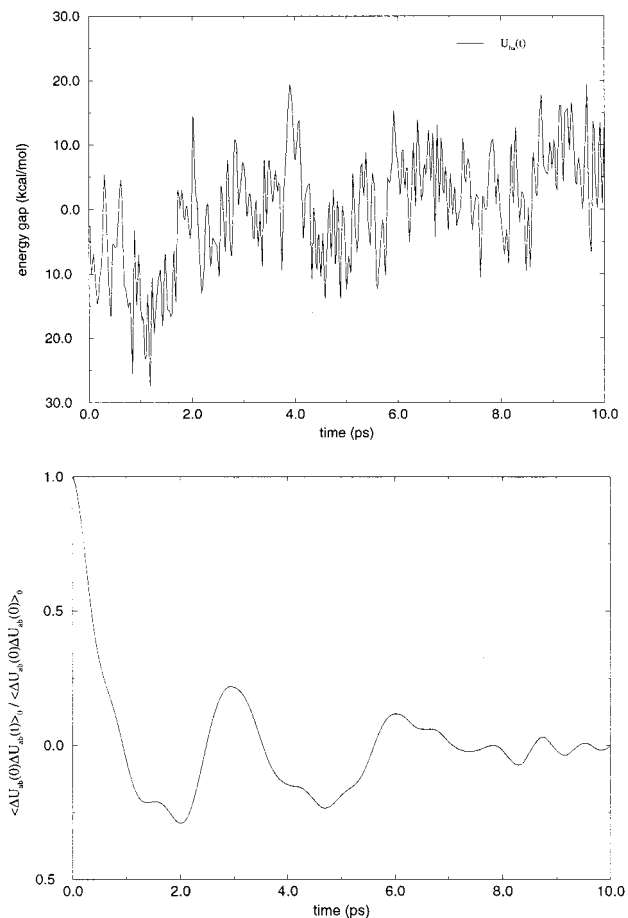


**Figure 1.** Fluctuations of the time-dependent energy gap (a) and the corresponding normalized autocorrelation function (b) for the  $\text{Na}^+ + \text{Na} \rightarrow \text{Na} + \text{Na}^+$  process considered in the text.

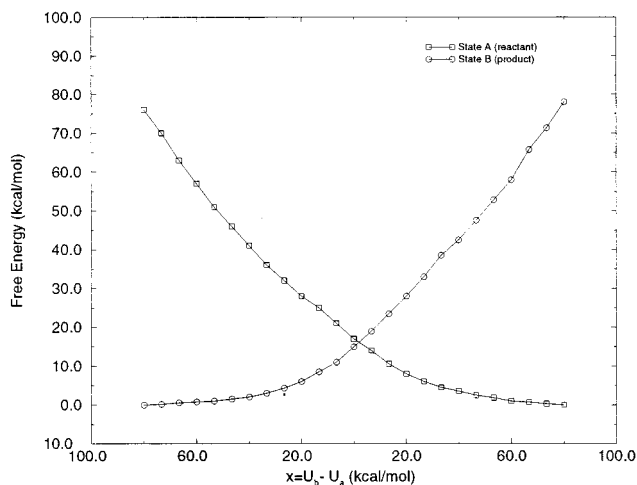


**Figure 2.** Free energy functions for the system considered in Figure 1. The reaction coordinate is taken as the energy gap (i.e.,  $x = U_b - U_a + (\epsilon_b^0 - \epsilon_a^0)$ , where  $(\epsilon_b^0 - \epsilon_a^0)$  is taken to be zero in this specific case). For a clear discussion of the nature of this reaction coordinate and the construction of the corresponding free energy functions  $g_a$  and  $g_b$ , see ref 20.

The free energy perturbation/umbrella sampling treatment gives the free energy functions (the Marcus parabola) depicted in Figure 2 with a reorganization energy  $\lambda = 75.0 \text{ kcal/mol}$ . The use of the energy gap  $\Delta U_{ba}(t)$  and the relationship  $\langle \Delta U_{ba} \rangle_a = \lambda + \Delta G_0$  gave  $\lambda = 75.4 \text{ kcal/mol}$ . The rate constant of our system was first estimated using the Marcus formula

$$k = |\sigma/\hbar|^2 [\pi\hbar^2/(k_B T \lambda)]^{1/2} \exp\{-\Delta g^\ddagger/(k_B T)\} \quad (30)$$

$$\Delta g^\ddagger = (\Delta G_0 + \lambda)^2/(4\lambda)$$

With the above  $\lambda$  and  $\sigma$  we obtain the dependence of the rate constant on  $\Delta G_0$  as described in Figure 3.

Next we examined our different density matrix treatments by comparing them to the Marcus rate constant. The calculations used the  $\Delta U_{ba}(t)$  of Figure 1 and produced time-dependent  $\rho$ 's of the type presented in Figure 4. The rate constant was calculated from the corresponding  $\rho(t)$  using

$$k = \frac{\Delta\langle\rho_{bb}(t)\rangle_0}{\Delta t} \quad (31)$$

where  $\Delta t$  is small on the reaction time scale but large on the time scale of the integration of  $\rho$ . The integration was done by the Runge–Kutta method.

The dependence of the rate constants of the different models on  $\Delta G_0$  was evaluated by repeating the calculations for different values of  $\epsilon_b^0 - \epsilon_a^0$ . We started this study by considering the performance of the semiclassical trajectory (ST) rate constant,  $k_{ST}$ , obtained from our previous surface hopping approach<sup>1,8</sup> (using the time dependence of the  $C$ 's of eq 4). The calculated  $k_{ST}$  (Figure 5) was obtained by the Runge–Kutta integration procedure with time steps of 0.2 fs. The results of this integration were averaged over 10 initial conditions. These initial conditions were generated by starting at different points along the simulated energy gap. As seen from Figure 5, our  $k_{ST}$  reproduces the results obtained by the Marcus relationship, as found in previous studies.<sup>1,8</sup> Next we examined the direct integration of the Liouville equation. In this case we needed time steps of 0.1 fs and an average of 20 initial conditions to obtain converged results that reproduced the results of Marcus' relationship (see Figure 5).

The performance of the second-order Liouville equation (eq 25) and the Redfield equation (eq 29) is described in Figure 6. The convergence of the second-order Liouville equation was obtained with time steps of 0.2 fs and an average of 20 initial conditions. The Redfield approach converged with time steps of 1.0 fs and an average of five initial conditions. Thus, it appears that the Redfield equation converges much more quickly than the direct integration of the Liouville equation and the second-order Liouville treatment. This is due to the use of the autocorrelation function, which is determined once and then used as a constant  $T_2$  term in the Redfield treatment. In our case we find that the Redfield treatment is roughly 20 times faster than the Liouville treatment.

In concluding this section, it might be useful to mention that all the treatments considered reproduce the correct microscopic reversibility. This is so, since all these treatments reproduced the trend obtained by the Marcus' relationship and this relationship involves forward and backward rate constants that satisfy the requirement of microscopic reversibility.

#### IV. Quantizing the Solvent Degrees of Freedom

The above treatments are based on a semiclassical approach that treats the solvent fluctuations classically. This involves several problems, ranging from the underestimate of quantum mechanical tunneling to the fact that the correct implementation of the semiclassical surface hopping approach is not necessarily clear. In fact, semiclassical approaches by their nature are not "exact" quantum mechanical treatments (see discussion in ref 8). There are also practical problems that are not fully resolved.

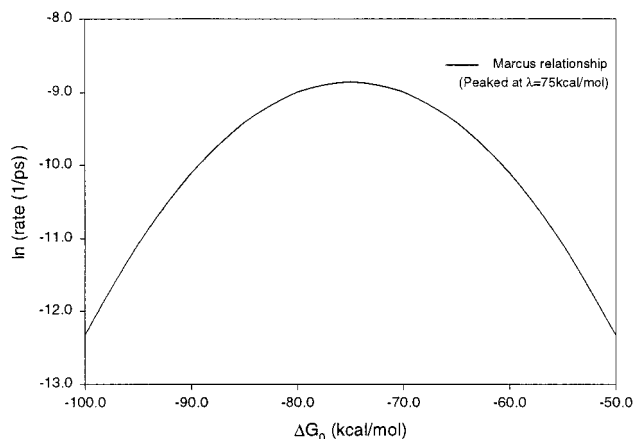


**Figure 3.** Rate constants for the  $\text{Na} + \text{Na}^+ \rightarrow \text{Na}^+ + \text{Na}$  type process as a function of an arbitrarily assumed  $\Delta G_0$ . The calculations were done using Marcus formula with the  $\lambda$  obtained from Figure 2 ( $\lambda = 75$  kcal/mol).

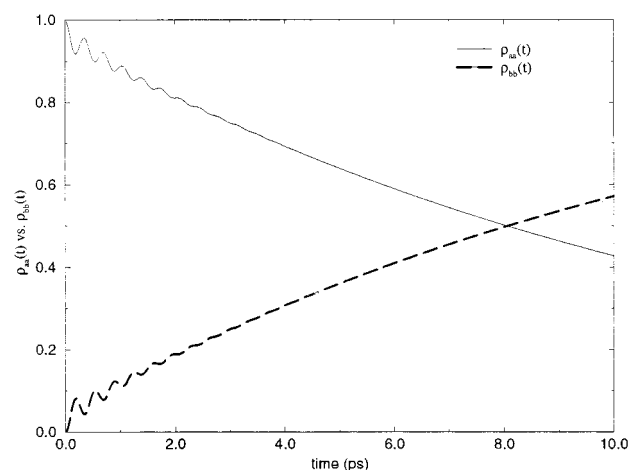


**Figure 4.** Typical time dependence of  $\rho_{aa}$  and  $\rho_{bb}$ . The results are taken from the Liouville equation treatment with  $\Delta G_0 = -75$  kcal/mol and  $\sigma = 1 \text{ cm}^{-1}$ .

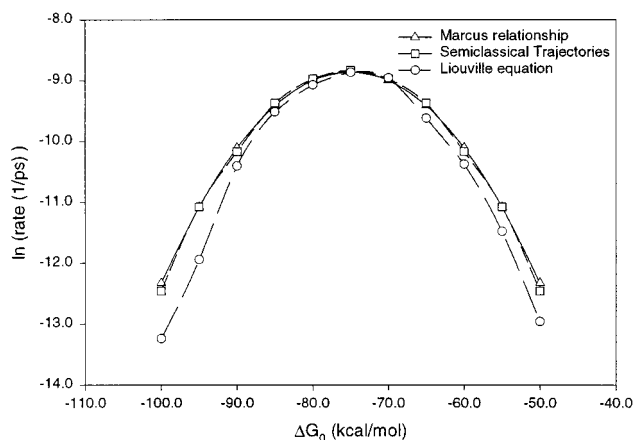


**Figure 5.** Dependence of the rate constants on  $\Delta G_0$  for the  $\text{Na} + \text{Na}^+ \rightarrow \text{Na}^+ + \text{Na}$  type process, calculated using the Liouville equation ( $\circ$ ), using the semiclassical trajectories approach ( $\square$ ), and using Marcus relationship ( $\triangle$ ). The calculations used  $\sigma = 1 \text{ cm}^{-1}$ .

For example, in our case it is not obvious what the correct way of treating the solute–solvent coupling should be. In the case of small electronic coupling, we can run trajectories on a potential surface that reflects only the reactant charges (see ref 8). However, when the magnitude of  $\sigma$  increases, it is more proper to let the solvent see a superposition of the reactant and

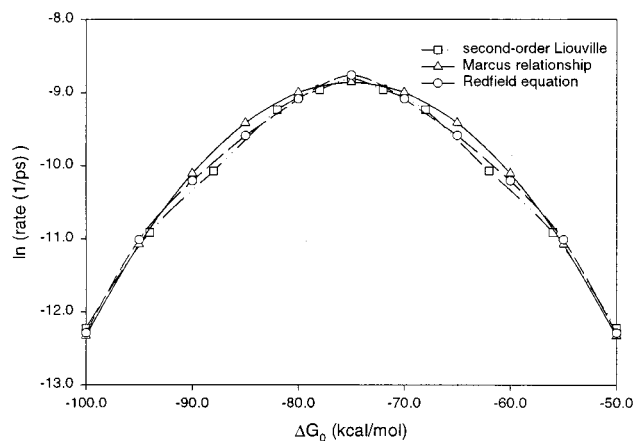


**Figure 6.** Dependence of the rate constant on  $\Delta G_0$  for the  $\text{Na} + \text{Na}^+ \rightarrow \text{Na}^+ + \text{Na}$  type reaction, calculated using the second-order Liouville equation ( $\square$ ) (eq 25), the modified Redfield equation ( $\circ$ ) (eq 29), and the Marcus relationship ( $\triangle$ ) (eq 30). The calculations used  $\sigma = 1 \text{ cm}^{-1}$ .

product charges (see ref 7) so that the solvent trajectories are propagated on a combination of the reactant and product potential surfaces. This can be partially solved by moving to the adiabatic representation, but the available formulations do not provide exact quantum mechanical results. Furthermore, approaches that involve splitting of trajectories are not easily implemented in Redfield type formulations.

A possible way to obtain a more rigorous quantum mechanical treatment that overcomes many of the above problems is to use vibronic-based density matrix approach. That is, one can try to develop approaches that treat the nuclear coordinate quantum mechanically but still reflect the microscopic physics of the simulated system. Thus, we divide our system into a quantum mechanical space that includes the solute modes and all the “active” solvent modes that are coupled to the solute reaction coordinate and a classical space that includes the rest of the solvent modes. For related work see refs 29–31. To treat the “active” solvent modes quantum mechanically, we have to know their vibrational frequencies and Franck–Condon (FC) factors. Fortunately, this can be accomplished using the dispersed polaron (spin boson) approach<sup>1,32</sup> where the FC factors for each pair of electronic states are obtained by considering the time-dependent energy gap as a Fourier transform,

$$\Delta U(t) = \frac{1}{2\pi} \int_{-\infty}^{\infty} A(\omega) e^{i\omega t} d\omega \quad (32)$$

Using the Wiener–Khinchine theorem, one obtains<sup>19</sup>

$$\lim_{\tau \rightarrow \infty} |A(\omega)|^2/\tau = \int dt e^{-i\omega t} \langle \Delta U(0) \Delta U(t) \rangle \quad (33)$$

Now using the relationship<sup>7</sup>

$$\langle \Delta U(0) \Delta U(t) \rangle = \hbar^2 \sum_s \omega_s^2 \Delta_s^2 (\bar{n}_s + 1/2) \cos \omega_s t \quad (34)$$

(where  $\Delta_j$  and  $\omega_j$  are, respectively, the origin shift and vibrational frequency of the  $s$ th state and  $\bar{n}_s = 1/[\exp(\hbar\omega_s\beta) - 1]$ ), one obtains<sup>8</sup>

$$\lim_{\tau \rightarrow \infty} |A(\omega)|^2/\tau = \pi \hbar \omega k_B T \sum_s \Delta_s^2 \delta(\omega - \omega_s) \quad (35)$$

where we use the high-temperature approximation for  $\bar{n}_s$ . Note that  $A(\omega)$  can be normalized by

$$\int_{-\infty}^{\infty} |A(\omega)|^2/\tau d\omega = \pi \hbar \omega \lambda^2 k_B T \quad (36)$$

where  $\lambda$  is the total reorganization energy. Once the origin shifts are known, we can get the FC factors by

$$c_{nm}^{\alpha\beta} = \prod_s c_{n_s, m_s}^{\alpha\beta} \quad (37)$$

where we use the relationship

$$(c_{n_s, 0}^{\text{ab}})^2 = \exp\{-\Delta_s^2/2\} \left(\frac{\Delta_s^2}{2}\right)^{n_s} / n_s! \quad (38)$$

and obtain the general  $c_{n_s, m_s}$  by using the proper recursion formula.<sup>8</sup>

With the solvent FC factors we can now write the vibronic Hamiltonian as

$$H_{nm}^{\alpha\beta} = \sigma_{\alpha\beta} c_{nm}^{\alpha\beta} \quad (39)$$

$$H_{nm}^{\alpha\alpha} = \sum_s \hbar \omega_s (n_s + 1/2)$$

Now we can write a Liouville equation for the system where, in contrast to the semiclassical case, we do not have any fluctuating term in our Hamiltonian (within the harmonic approximation). This means that, at least formally, we have no  $T_2$  term of the type given by eq 28 and all the corresponding dissipation effects are given by the  $c_{nm}$  terms (which provide the equivalent of the  $T_2$  term). However, our treatment requires a term that represents the dissipation of energy between vibrations of the same electronic state. That is, our Liouville equation is expressed as

$$\langle \dot{\rho} \rangle = \langle \rho \mathbf{H} - \mathbf{H} \rho + \mathbf{R}(\rho - \rho^{\text{eq}}) \rangle \quad (40)$$

where  $\rho^{\text{eq}}$  is the equilibrium value of  $\rho$ , while  $\mathbf{R}$  is the relaxation matrix. In our case, we choose the simple expression

$$R_{nm}^{\alpha\beta} = 0 \quad \text{for } \alpha \neq \beta \quad (41)$$

$$R_{nm}^{\alpha\alpha} = -\frac{1}{T_1} \quad \text{for } \sum_s |m_s - n_s| = 1$$

$$R_{nm}^{\alpha\alpha} = 0 \quad \text{for } \sum_s |m_s - n_s| > 1$$

We could, of course, use more rigorous expressions (e.g., ref 30), which will be examined in subsequent studies. However, the main point is that  $T_1$  is still a phenomenological parameter (microscopic strategies for obtaining  $T_1$  will be considered in subsequent work). Thus, the present treatment describes the relaxation between different electronic states (the  $T_2$  process) by the microscopically derived  $\sigma_{\alpha\beta} c_{nm}^{\alpha\beta}$  terms of eq 39, while describing the relaxation within vibronic levels of the same electronic states using a phenomenological  $T_1$ .

To examine the vibronic approach, we considered the electron transfer from the bacteriochlorophyll chromophore ( $H_L$ ) to the primary quinone ( $Q_A$ ) in the bacterial reaction center of *Rps. viridis* (see ref 1 for a description of this system). This process was studied previously by a dispersed polaron treatment.<sup>21</sup> The present work represented the  $\Delta_s(\omega)$  of ref 21 by a three-mode model, using  $\Delta_1 = 1.10$ ,  $\Delta_2 = 1.80$ ,  $\Delta_3 = 1.84$ ,  $\omega_1 = 40 \text{ cm}^{-1}$ ,  $\omega_2 = 400 \text{ cm}^{-1}$  and  $\omega_3 = 2275 \text{ cm}^{-1}$ .  $T_1$  was taken as 1 ps following ref 1. The vibronic Liouville equation that was constructed for the assumed  $\Delta G^{\circ}$  (values between zero to

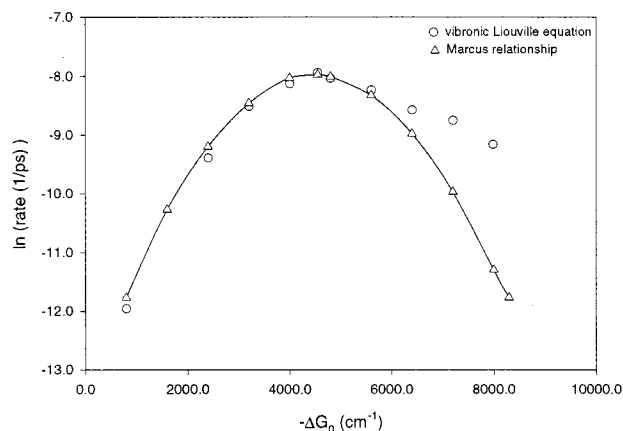


**Figure 7.** Comparison between the Marcus relationship ( $\Delta$ ) and the vibronic Liouville equation ( $\circ$ ).

$-10\,000\text{ cm}^{-1}$ ) and the corresponding rate constants were calculated by direct integration of this equation. The dependence of the calculated rate constant on  $\Delta G^\circ$  is shown in Figure 7. As can be seen by comparing Figure 7 to Figure 4b of ref 21, we reproduce the general trend of the dispersed polaron treatment and in particular the deviation from the Marcus relationship in the inverted region.

## V. Concluding Remarks

This work developed and examined microscopically based density matrix methods for studies of electron transfer and other charge-transfer reactions in condensed phases. The starting point of our approach is a molecular dynamics simulation of a donor-acceptor pair in an all-atom solvent model. The simulation provides the time-dependent gap between the energies of the product and reactant states, and this energy gap is introduced in the diagonal elements of the Hamiltonian of the system. The resulting time-dependent Hamiltonian is then used to construct the corresponding Liouville equation. This Liouville equation is then used in three treatments. The first one involves a direct numerical integration of the Liouville equation. The second treatment manipulates the second-order Liouville equation in the way used in the derivation of the Redfield equation. The resulting second-order equation is then integrated numerically. The third approach constructs a Redfield type equation directly using the Redfield formulation for the various matrix elements and adding the effect of the time-independent electronic matrix element. The resulting equation is then integrated numerically.

The validity of the different treatments is examined by comparing their results to those obtained from the corresponding Marcus equation. All the methods reproduce the results obtained from the Marcus equation. However, the direct integration of the Liouville equation and the second-order Liouville equation converge much more slowly than the Redfield treatment.

Having a microscopically based density matrix can provide an interesting insight. For example, in the present case we obtain the autocorrelation time  $T_2$  directly from the autocorrelation of the electronic energy gap. This is quite different from treatments that consider  $T_2$  as a phenomenological parameter. This point is particularly important in studies of ET in proteins where it is not obvious how to obtain the proper value of  $T_2$  without relating it to microscopic simulation of the actual environment around the donor and acceptor.

Our treatments can be used, at least formally, in both the diabatic and adiabatic limits. In the diabatic limit we can run trajectories on the reactant state and assume that those trajectories that cross to the product state will not cross back in a

short time. We can also assume that trajectories that cross to the product surface do not interfere with those that move on the reactant surface. Unfortunately, the issue of what is the effective surface for the nuclear trajectories (the solvent trajectories) is less clear, despite recent advances (for example, see ref 22). Furthermore, in the adiabatic limit we have to consider the proper solute-solvent coupling. It is possible that using the current approach for large  $\sigma$  will produce results that do not obey microscopic reversibility. In such cases one may require the solute to follow a potential that involves the adiabatic solute dipole.<sup>7</sup> Examination of this important issue is left to subsequent studies.

The main focus of the present work was placed on a semiclassical treatment where the solvent coordinates are considered classically. Such a treatment is subject to the above-mentioned problems. Furthermore, quantum mechanical features of the solvent motion are neglected. These problems can be overcome, at least in a partial way, by using an alternative approach<sup>1</sup> that treats the solvent motion quantum mechanically. In this approach we follow the same trick introduced in the dispersed polaron (spin boson) model<sup>8,32</sup> and use molecular simulations to evaluate the Franck-Condon factors for the solvent modes. These Franck-Condon factors are then introduced in the relevant Liouville equation.<sup>1</sup> Here again, we have a microscopically based density matrix with the exception that the correlation time  $T_1$  for transition between vibrations in the same electronic manifold is considered as a phenomenological parameter. Future studies will attempt to obtain this parameter from microscopic simulations.

**Acknowledgment.** This work was supported by NIH Grant GM40283.

## References and Notes

- (1) Warshel, A.; Parson, W. W. *Annu. Rev. Phys. Chem.* **1991**, *42*, 279.
- (2) Warshel, A. *Computer Modeling of Chemical Reactions in Enzymes and Solutions*; John Wiley & Sons: New York, 1991.
- (3) Barbara, P. F.; Meyer, T. J.; Ratner, M. A. *J. Phys. Chem.* **1996**, *100*, 13148.
- (4) Newton, M. *Chem. Rev.* **1991**, *91*, 767.
- (5) Marcus, R. A.; Sutin, N. *Biochim. Biophys. Acta.* **1985**, *811*, 263.
- (6) Warshel, A. *J. Phys. Chem.* **1982**, *86*, 2218.
- (7) Hwang, J.-K.; King, G.; Creighton, S.; Warshel, A. *J. Am. Chem. Soc.* **1988**, *110*, 5297.
- (8) Warshel, A.; Hwang, J.-K. *J. Chem. Phys.* **1986**, *84*, 4938.
- (9) Neria, E.; Nitzen, A. *Chem. Phys.* **1994**, *183*, 351.
- (10) Kuharski, R. A.; Bader, J. S.; Chandler, D.; Sprik, M.; Klein, M. L.; Impey, R. W. *J. Chem. Phys.* **1988**, *89*, 3248.
- (11) Zheng, C.; McCammon, J. A.; Wolynes, P. G. *Proc. Natl. Acad. Sci. U.S.A.* **1989**, *86*, 6441.
- (12) Schulten, K.; Tesch, M. *Chem. Phys.* **1991**, *158*, 421.
- (13) Lobaugh, J.; Voth, G. A. *J. Chem. Phys.* **1996**, *104*, 2056.
- (14) (a) Hwang, J.-K.; Warshel, A. *J. Am. Chem. Soc.* **1996**, *118*, 11745. (b) Hwang, J.-K.; Chu, Z. T.; Yadav, A.; Warshel, A. *J. Phys. Chem.* **1991**, *95*, 8445. (c) Warshel, A.; Chu, Z. T. *J. Phys. Chem.* **1990**, *93*, 4003.
- (15) (a) Vuilleumier, R.; Borgis, D. *Chem. Phys. Lett.* **1998**, *284*, 71. (b) Vuilleumier, R.; Borgis, D. *J. Phys. Chem.* **1998**, *102*, 4261.
- (16) Hammes-Schiffer, S.; Tully, J. C. *J. Phys. Chem.* **1995**, *99*, 5793.
- (17) Slichter, C. P. *Principles of Magnetic Resonance*; Springer-Verlag: Berlin, 1978.
- (18) Jean, J. M.; Friesner, R. A.; Fleming, G. R. *J. Chem. Phys.* **1992**, *96*, 5827.
- (19) Figueirido, F. E.; Levy, R. M. *J. Chem. Phys.* **1992**, *97*, 703.
- (20) King, G.; Warshel, A. *J. Chem. Phys.* **1989**, *91*, 3647.
- (21) Warshel, A.; Chu, Z. T.; Parson, W. W. *Science* **1989**, *246*, 112.
- (22) Webster, F.; Rossky, P. J.; Friesner, R. A. *Comput. Phys. Comm.* **1991**, *63*, 494.
- (23) Wolfseder, B.; Domcke, W. *Chem. Phys. Lett.* **1996**, *259*, 113.
- (24) Evans, D. G.; Nitzen, A.; Ratner, M. A. *J. Chem. Phys.* **1998**, *108*, 6387.
- (25) Laird, B. B.; Skinner, J. L. *J. Chem. Phys.* **1991**, *94*, 4405.
- (26) Kavanaugh, T. C.; Silbey, R. J. *J. Chem. Phys.* **1993**, *98*, 9444.

- (27) Ashkenazi, G.; Kosloff, R.; Ratner, M. A. *J. Am. Chem. Soc.* **1999**, *121*, 3386.
- (28) Budimir, J.; Skinner, J. L. *J. Stat. Phys.* **1987**, *49*, 1029.
- (29) May, V.; Kuhn, O.; Schreiber, M. *J. Phys. Chem.* **1993**, *97*, 12591.
- (30) Jean, J. M.; Fleming, G. R. *J. Chem. Phys.* **1995**, *103*, 2092.
- (31) Matro, A.; Cina, J. A. *J. Phys. Chem.* **1995**, *99*, 2568.
- (32) Hwang, J.-K.; Warshel, A. *Chem. Phys. Lett.* **1997**, *271*, 223.
- (33) Luzhkov, V.; Warshel, A. *J. Am. Chem. Soc.* **1991**, *113*, 4491.
- (34) Lee, F. S.; Chu, Z. T.; Warshel, A. *J. Comput. Chem.* **1993**, *14*, 161.
- (35) Sham, Y. Y.; Muegge, I.; Warshel, A. *Biophys. J.* **1998**, *74*, 1744.
- (36) Lee, F. S.; Warshel, A. *J. Chem. Phys.* **1992**, *97*, 3100.